iScience

CellPress
OPEN ACCESS

Article

Hypoxia induces hepatocellular carcinoma metastasis via the HIF-1α/METTL16/lnc-CSMD1-7/RBFOX2 axis

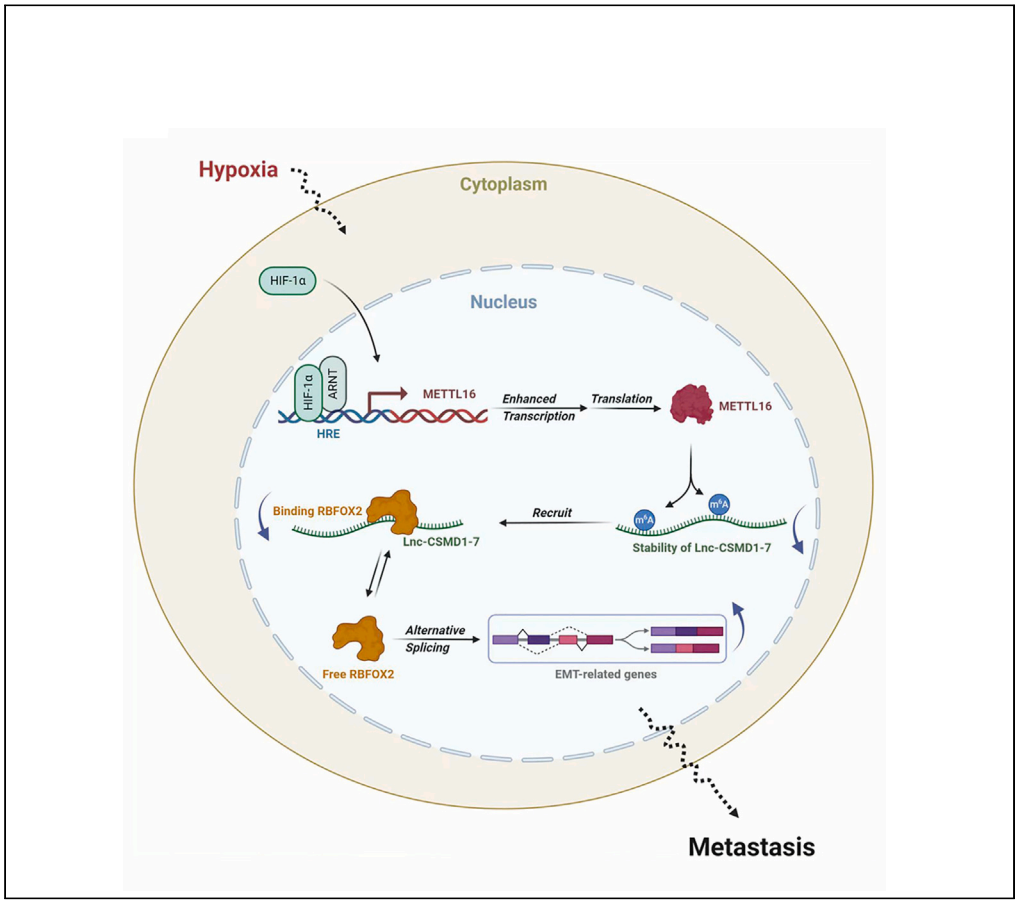

Yingchao Wang, Yong Yang, Ye Yang, ..., Xiaolong Liu, Wuhua Guo, Bixing Zhao

xiaoloong.liu@gmail.com (X.L.)
guowuhua@aliyun.com (W.G.)
bixingzhao@gmail.com (B.Z.)

Highlights

Lnc-CSMD1-7 is downregulated in HCC and associated with poor prognosis

Lnc-CSMD1-7 suppresses HCC metastasis *in vitro* and *in vivo*

Lnc-CSMD1-7 binds to RBFOX2 and affects alternative splicing of EMT-related genes

Hypoxia regulates HCC metastasis through HIF-1α/METTL16/Lnc-CSMD1-7/RBFOX2 axis

Wang et al., iScience *26*, 108495
December 15, 2023
https://doi.org/10.1016/j.isci.2023.108495

iScience

CellPress
OPEN ACCESS

Article

Hypoxia induces hepatocellular carcinoma metastasis via the HIF-1α/METTL16/lnc-CSMD1-7/RBFOX2 axis

Yingchao Wang,[1,2,5] Yong Yang,[1,2,4,5] Ye Yang,[1,2,5] Yuan Dang,[4,5] Zhiting Guo,[1,2] Qiuyu Zhuang,[1,2] Xiaoyuan Zheng,[1] Fei Wang,[1] Niangmei Cheng,[1] Xiaolong Liu,[1,2,*] Wuhua Guo,[2,3,*] and Bixing Zhao[1,2,6,*]

SUMMARY

Hypoxic microenvironment is clinically associated with metastasis and poor prognosis of numerous cancers. The mechanisms by which intratumoral hypoxia regulates metastasis are not fully understood. Our study identifies a downregulation of Lnc-CSMD1-7 in hepatocellular carcinoma (HCC) and correlated with poor prognosis of HCC patients. Lnc-CSMD1-7 negatively regulated HCC cell migration and invasion *in vitro* and suppressed lung metastasis *in vivo*. Mechanistically, Lnc-CSMD1-7 directly binds to RBFOX2, thereby affecting RBFOX2-regulated alternative splicing in epithelial and mesenchymal-specific events. More importantly, hypoxic microenvironment and m6A methylation mediate the downregulation of Lnc-CSMD1-7 expression. Specifically, hypoxia transcriptionally upregulates the expression of the m6A methyltransferase METTL16 via HIF-1α, and METTL16 directly binds to Lnc-CSMD1-7 and downregulates the RNA stability of Lnc-CSMD1-7 via m6A methylation, ultimately promoting HCC metastasis. Our findings highlight the regulatory function of the METTL16/Lnc-CSMD1-7/RBFOX2 axis in modulating hypoxia-induced HCC progression, which may provide potential prognostic and therapeutic targets for HCC treatment.

INTRODUCTION

Hepatocellular carcinoma (HCC) remains one of the most common malignancies and accounts for the third leading cause of cancer-related death worldwide.[1] The 5-year survival rate of patients with HCC remains low due to late diagnosis, post-surgical metastasis, and recurrence. Therefore, there is an urgent need to elucidate the detailed molecular mechanisms involved in HCC tumorigenesis and progression and discover more effective treatment targets for HCC.

Hypoxia is a hallmark feature of the tumor microenvironment and a potent microenvironmental factor promoting metastatic progression.[2] Hypoxia-inducible factor-1α (HIF-1α) is a key transcription factor that is induced by hypoxia via the promotion of HIF-1αprotein stability.[3] Due to the proliferative nature of HCC, hypoxia is often found in regions of the HCC tumor tissue. Hypoxia can trigger a number of pro-metastatic molecular events in HCC and worsen prognosis. Studies show that HIF-1α is highly expressed and significantly associated with advanced stage and aggressive phenotypes in HCC.[4] Understanding the role of hypoxia in HCC metastasis may facilitate the development of new therapeutic strategies for advanced HCC. However, the exact mechanisms involved in hypoxia-driven HCC metastasis are not well understood.

Long non-coding RNAs (lncRNAs) are transcripts that are longer than 200 bp and lack protein-coding potential. Accumulating evidence indicates that lncRNAs exert regulatory roles at almost all stages of gene expression, from targeting epigenetic modification, transcriptional regulation, and interactions of lncRNAs-proteins, lncRNAs-miRNAs-mRNAs, and lncRNA-lncRNA.[5] LncRNA-protein interactions functioned as a vital mechanism of lncRNAs in HCC. LncRNA-LET associates with NF90 to enhance the degradation of NF90, therefore inhibits HCC metastasis.[6] LncHOXA10 recruits SNF2L to its promoter to initiate the expression of HOXA10, therefore promotes the self-renewal of liver tumor initiating cells and liver tumorigenesis.[7] Despite these studies, the role of lncRNA-protein interactions in the tumorigenesis and development of HCC remains to be further investigated.

As the most common internal modification of mammalian messenger RNAs, n6-methyladenosine (m6A) plays an important role in normal biological processes and development by regulating the fate of target RNAs, and its aberrant regulation has been implicated in a variety of

[1]The United Innovation of Mengchao Hepatobiliary Technology Key Laboratory of Fujian Province, Mengchao Hepatobiliary Hospital of Fujian Medical University, Fuzhou 350025, P.R. China
[2]Mengchao Med-X Center, Fuzhou University, Fuzhou 350116, P.R. China
[3]Department of Interventional Radiology, Mengchao Hepatobiliary Hospital of Fujian Medical University, Fuzhou, Fujian, China
[4]Fujian Medical University Cancer Hospital, Fujian Cancer Hospital, Fuzhou, China
[5]These authors contributed equally
[6]Lead contact
*Correspondence: xiaoloong.liu@gmail.com (X.L.), guowuhua@aliyun.com (W.G.), bixingzhao@gmail.com (B.Z.)
https://doi.org/10.1016/j.isci.2023.108495

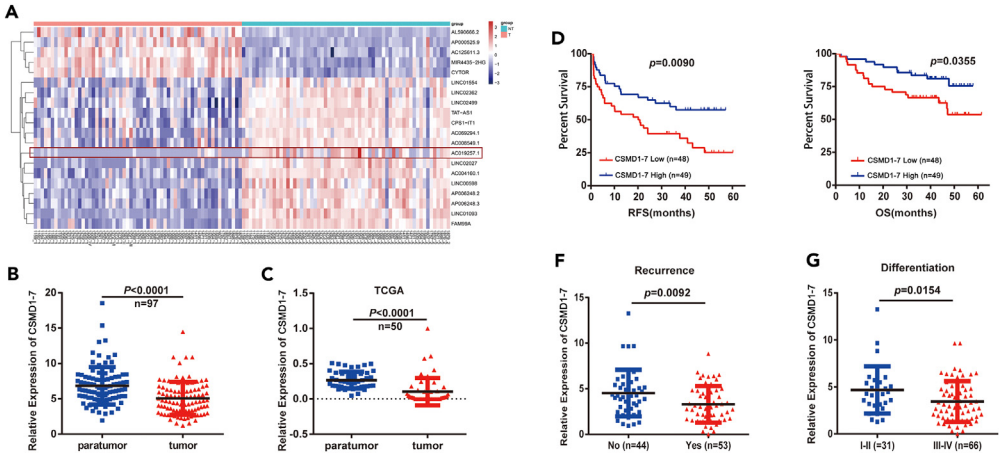

Figure 1. LncRNA-Lnc-CSMD1-7 was downregulated in HCC and correlated with poor prognosis

(A) Heatmap of the top 20 dysregulated lncRNAs in 61 paired HCC tumor and adjacent paratumor tissues.

(B) RT-qPCR validation of Lnc-CSMD1-7 expression in 97 HCC patients with paired tumor and paratumor tissues.

(C) Relative expression of Lnc-CSMD1-7 in 50 HCC tissues obtained from the TCGA database.

(D and E) Kaplan-Meier analysis showed that low expression of Lnc-CSMD1-7 was significantly associated with shorter RFS (D) and OS (E).

(F) Relative expression of Lnc-CSMD1-7 in HCC patients with or without recurrence.

(G) Differential expression levels of Lnc-CSMD1-7 in HCC patients with stage I—II and stage III-IV differentiation.

diseases, including cancer.[8] METTL16 was recently identified as an m6A methyltransferase and was found to regulate tumor initiation and development through its m6A methylation function. METTL16 exerts its oncogenic role by promoting the expression of branched-chain amino acid transaminase 1 (BCAT1) and BCAT2 in an m6A-dependent manner and drives leukemogenesis and leukemia stem cell self-renewal.[9] METTL16 promotes HCC progression by downregulating RAB11B-AS1 in an m6A-dependent manner.[10] However, the role of METTL16 and its modified RNA substrates in tumor remains to be further investigated.

Alternative splicing (AS), an important post-transcriptional process, is a key mechanism for modulating gene function and gives rise to diverse messenger RNA (mRNA) isoforms through different arrangements of exons within precursor mRNAs.[11] As a key process in tumor metastasis, epithelial-mesenchymal transition (EMT) is regulated by both alternative splicing and transcriptional regulation.[12] These alternative splicing events are controlled by various splicing factors, including RBFOX2.[13,14] In pancreatic ductal adenocarcinoma, RBFOX2 acts as a tumor suppressor to modulate a metastatic signature of alternative splicing.[15] In endometrial cancer, circRAPGEF5 promotes the formation of exon-4 skipping TFRC and confers ferroptosis resistance by inhibiting the binding of RBFOX2 to pre-mRNA.[16] However, the role of aberrant AS and RBFOX2 in HCC has not been elucidated.

Lnc-CSMD1-7(AC019257.1) is a lncRNA that is located at chromosome 8p23.3, and there have been no studies on its function. In this study, we found that Lnc-CSMD1-7 was dramatically downregulated in HCC tissues, and lower expression of Lnc-CSMD1-7 correlated with poor prognosis. Gain-and loss-of function studies reveal that Lnc-CSMD1-7 negatively regulates invasion and migration of HCC cells. Mechanistically, METTL16-mediated m6A modification reduces the stability of Lnc-CSMD1-7, and Lnc-CSMD1-7 binds to RBFOX2 and affects alternative splicing in epithelial and mesenchymal-specific events. More importantly, our study elucidated the regulatory role of the hypoxic microenvironment on Lnc-CSMD1-7 and METTL16. In conclusion, our current studies demonstrated the key functions of Lnc-CSMD1-7 in hypoxia-induced HCC metastasis. The present study may provide new insights and further understanding into the underlying mechanisms of hypoxia promoted metastasis and reveal that Lnc-CSMD1-7 could be a potential target for the development of new anticancer strategies in hypoxia-related cancers.

RESULTS

LncRNA-Lnc-CSMD1-7 was downregulated in HCC and correlated with poor prognosis

To identify the potential key long non-coding RNA associated with HCC, lncRNA sequencing analysis was performed in 61 paired HCC tissues and corresponding paratumor tissues. The top 20 differentially expressed lncRNA were shown in the heatmap (Figure 1A). Among them, Lnc-CSMD1-7 (AC019257.1) was one of the downregulated lncRNAs in HCC tissues. So far, the study of Lnc-CSMD1-7 has not been reported, so we focused on this uncharacterized lncRNAs. To further verify the downregulation of Lnc-CSMD1-7 in HCC, we examined its level in 97 pairs of HCC and matched normal tissue samples by qRT-PCR. A dramatic downregulation of Lnc-CSMD1-7 was observed in HCC tissues compared to normal tissues (Figure 1B). The downregulation of Lnc-CSMD1-7 was also observed in the TCGA dataset (Figure 1C).

Notably, when we examined the prognostic values of Lnc-CSMD1-7 in HCC patients using Kaplan-Meier plot, it showed that low expression level of Lnc-CSMD1-7 was associated with shorter recurrence-free survival (RFS) and overall survival (OS) in HCC patients (Figures 1D and 1E). This result is also confirmed by TCGA data (Figure S1). Further clinical pathology data analysis shows that the

Table 1. Association between Lnc-CSMD1-7 expression and clinicopathological features of HCC patients (n = 97)

	Lnc-CSMD1-7 expression		
Clinical characteristics	Low (48)	High (49)	p value
Sex			
Male	42	39	0.294
Female	6	10	
Age (years)			
≤55	26	22	0.361
> 55	22	27	
Tumor size (cmv)			
< 5	23	28	0.363
≥5	25	21	
Tumor number			
Single	48	47	0.368
Multiple	0	2	
HCC stage, BCLC			
0-A	43	43	0.845
B-C	5	6	
TNM			
I—II	38	38	0.847
III—IV	10	11	
AFP (ng/mL)			
< 400	33	35	0.773
≥400	15	14	
Tumor differentiation			
I—II	10	21	**0.02***
III—IV	38	28	
Tumor metastasis			
Yes	0	3	0.082
No	48	46	
Recurrence			
Yes	33	20	**0.006****
No	15	29	
Tumor envelope			
Yes	42	44	0.721
No	6	5	
Tumor boundary			
Yes	41	44	0.513
No	7	5	
Microvascular invasion			
Positive	24	31	0.187
Negative	24	18	

*p < 0.05, **p < 0.01.

expression level of Lnc-CSMD1-7 was lower in recurrence than in non-recurrence patients (p = 0.0092). Meanwhile, patients with III-IV differentiation also showed lower expression of Lnc-CSMD1-7 (p = 0.0154) (Table 1; Figures 1F and 1G). Univariate and multivariate Cox regression analysis showed that low expression of Lnc-CSMD1-7 served as an independent prognostic factor for overall survival of HCC

Table 2. Univariate and multivariate cox regression analysis affecting overall survival of HCC patients

Variables	Case number	HR (95% CI)	*p* value
Univariate analysis			
Lnc-CSMD1-7 (Low vs. High)	48 vs. 49	0.440 (0.204–0.947)	0.036*
Gender (Male vs. Female)	81 vs. 16	0.848 (0.322–2.231)	0.738
Age (>55 vs. ≤ 55)	49 vs. 48	0.466 (0.216–1.002)	0.051*
Tumor size (<5 vs. ≥ 5)	51 vs. 46	6.074 (2.463–14.974)	0.0001***
Tumor number (Single vs. Multiple)	95 vs. 2	0.274 (0.002–41.608)	0.613
TNM (III/IV vs. I/II)	21 vs. 76	4.244 (2.012–8.951)	0.0001***
AFP (<400 vs. ≥ 400)	68 vs. 29	2.200 (1.056–4.584)	0.035*
Tumor margin (Clear vs. Obscure)	84 vs. 13	0.267 (0.113–0.632)	0.003**
Tumor capsule (Yes vs. No)	86 vs. 11	0.365 (0.148–0.899)	0.029*
Cirrhosis (Yes vs. No)	77 vs. 20	1.410 (0.537–3.703)	0.485
Tumor differentiation (III/IV vs. I/II)	66 vs. 31	2.844 (1.083–7.466)	0.034*
Multivariate analysis			
Lnc-CSMD1-7 (Low vs. High)	48 vs. 49	0.333 (0.147–0.753)	0.008**
Tumor size (<5 vs. ≥ 5)	51 vs. 46	4.212 (1.590–11.157)	0.004**
TNM (III/IV vs. I/II)	21 vs. 76	3.135 (1.338–7.345)	0.009**

*p < 0.05, **p < 0.01, ***p < 0.001.

patients (Table 2). Therefore, these data suggest that reduced tumor Lnc-CSMD1-7 levels are associated with poor clinical outcomes in HCC patients.

Lnc-CSMD1-7 suppresses HCC metastasis *in vitro* and *in vivo*

We next sought to determine the effect of Lnc-CSMD1-7 on the phenotype of HCC cells. First, we stably overexpressed Lnc-CSMD1-7 in SMMC-7721 cell lines and knocked down Lnc-CSMD1-7 in SNU-449 and SK-Hep-1 cell lines, and Figure 2A shows the overexpression and knock-down effects of Lnc-CSMD1-7.

The effect of Lnc-CSMD1-7 on HCC cell migration and invasion was examined using transwell assays. As shown in Figures 2B and 2C, ectopic expression of Lnc-CSMD1-7 significantly suppressed the migration and invasion of SMMC-7721 cells. Conversely, knockdown of Lnc-CSMD1-7 in SNU-449 cells had the opposite effect. Furthermore, loss of Lnc-CSMD1-7 decreased the protein level of the epithelial marker E-cadherin while increasing the expression of mesenchymal markers such as N-cadherin and vimentin (Figure 2D). We further investigated the effect of Lnc-CSMD1-7 on HCC metastasis *in vivo*. SMMC-7721 cells overexpressing Lnc-CSMD1-7 or corresponding control cells and SK-Hep-1 cells knocking down Lnc-CSMD1-7 or corresponding control cells were injected into mice via the tail vein. 4 weeks after injection, mice injected with Lnc-CSMD1-7-overexpressing cells showed significantly reduced HCC lung metastasis, as shown by bioluminescence imaging (Figure 2E). The number of metastatic colonies in the control group indicated increased invasion compared to the Lnc-CSMD1-7 overexpression group. Conversely, knockdown of Lnc-CSMD1-7 in SK-Hep-1 cells had the opposite effects (Figures 2E–2G). Histological analysis by H&E staining of the dissected lungs confirmed that the control group had more metastatic nodules than the Lnc-CSMD1-7-overexpression group (Figure 2G). Taken together, these results indicate the critical role of Lnc-CSMD1-7 in suppressing HCC metastasis.

Lnc-CSMD1-7 suppresses EMT by sequestering RBFOX2 protein in HCC

To further explore the molecular mechanism of Lnc-CSMD1-7 in regulating HCC metastasis, we first detected the subcellular localization of Lnc-CSMD1-7 by subcellular fractionation assay and *in situ* hybridization assay, and the results showed that Lnc-CSMD1-7 was mainly located in the nucleus of HCC cells (Figures 3A and 3B). LncRNAs are reported to exert their functions through interacting with RNA binding proteins (RBPs), which regulate gene expression by various mechanisms.[17] Therefore, we speculated that Lnc-CSMD1-7 may regulate HCC metastasis by interacting with specific RBPs.

To test this theory, RNA-pull down/MS was performed to identify Lnc-CSMD1-7 interacting proteins (Figure 3C). Among the candidates that interacted with Lnc-CSMD1-7, we noticed that RBFOX2, which is a regulator of alternative splicing, has been reported to promote the mesenchymal tissue-specific splicing pattern and promote EMT.[14] Therefore, we further confirmed the interaction between Lnc-CSMD1-7 and RBFOX2 by RNA-pull down/western blot and RIP/qRT-PCR (Figures 3D and 3E).

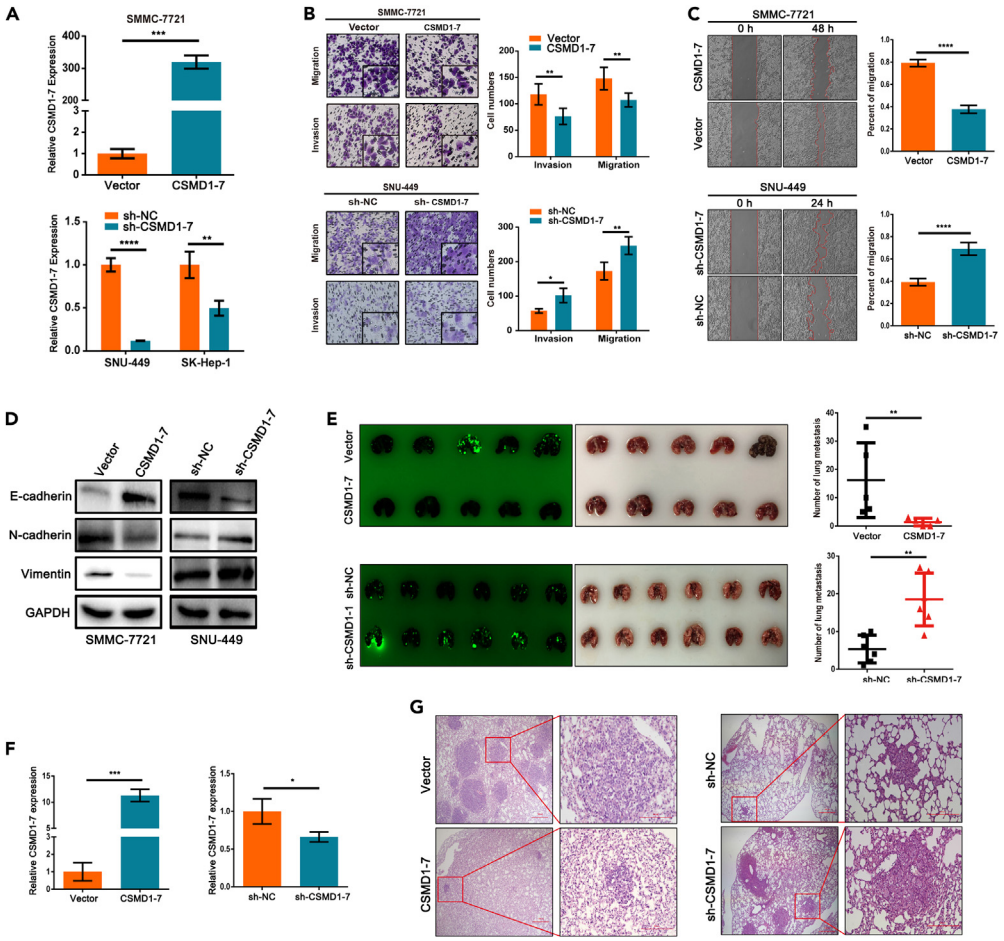

Figure 2. Lnc-CSMD1-7 suppresses HCC metastasis in vitro and in vivo

(A) The overexpression effect of Lnc-CSMD1-7 in SMMC-7721 cells and the knockdown effect of Lnc-CSMD1-7 in SNU-449 and SK-Hep-1 cells.

(B) Representative and quantification results of transwell cell migration and invasion assay in Lnc-CSMD1-7 overexpressed SMMC-7721 cells and Lnc-CSMD1-7 knocked down SNU-449 cells.

(C) Representative and quantification results of wound healing assay in Lnc-CSMD1-7 overexpressed SMMC-7721 cells and Lnc-CSMD1-7 knocked down SNU-449 cells.

(D) Western blotting detection of E-cadherin, N-cadherin and vimentin in Lnc-CSMD1-7 overexpressed SMMC-7721 cells and Lnc-CSMD1-7 knocked down SNU-449 cells, respectively.

(E) Representative images and quantification data of metastatic nodules in the mouse lung tissues. Stable cell lines of Lnc-CSMD1-7 overexpression or knockdown were injected into the tail vein of B-NSG mice.

(F) Overexpression and knockdown effect of Lnc-CSMD1-7 in metastatic nodules.

(G) Representative images of lung metastatic nodules stained with H&E.

Scale bar: 500 μm. Graph data were presented as mean ± SEM. *p < 0.05,**p < 0.01, ***p < 0.001, ****p < 0.0001 (Student's *t* test).

To verify the ability of Lnc-CSMD1-7 to suppress HCC metastasis in an RBFOX2-dependent manner, Lnc-CSMD1-7 stably overexpression cells or their control cells were transiently transfected with RBFOX2 overexpression vector or the corresponding empty vector, respectively. Restoration experiments showed that RBFOX2 overexpression attenuated the role of Lnc-CSMD1-7 overexpression in enhancing the migration and invasion of HCC cells (Figures S2 and 3F). Furthermore, RBFOX2 overexpression correspondingly reversed the effects of Lnc-CSMD1-7 on the expression of E-cadherin, N-cadherin, and Vimentin, indicating that Lnc-CSMD1-7 inhibits HCC EMT via an RBFOX2-dependent manner (Figure 3G). Studies have shown that, during EMT, Rbfox2-regulated splicing shifts from epithelial- to mesenchymal-specific events, including inclusion of the exon 13 of the *Slk* mRNA, inclusion of exon 11 of the *Cttn* mRNA, and skipping of the 12-nt exon of the *Dnm2* mRNA.[13] Therefore, three RBFOX2 targets were selected to verify the influence of Lnc-CSMD1-7 on RBFOX2-regulated splicing. The results showed that Lnc-CSMD1-7 knockdown decreased the alternative exon inclusion of the Slk transcript. Meanwhile, the skipping of the 12-nt exon of *Dnm2* transcripts and the inclusion of *Cttn* exon 11 were significantly upregulated (Figure 3H) indicating that Lnc-CSMD1-7 inhibits Rbfox2-regulated splicing shifts from epithelial- to mesenchymal-specific events.

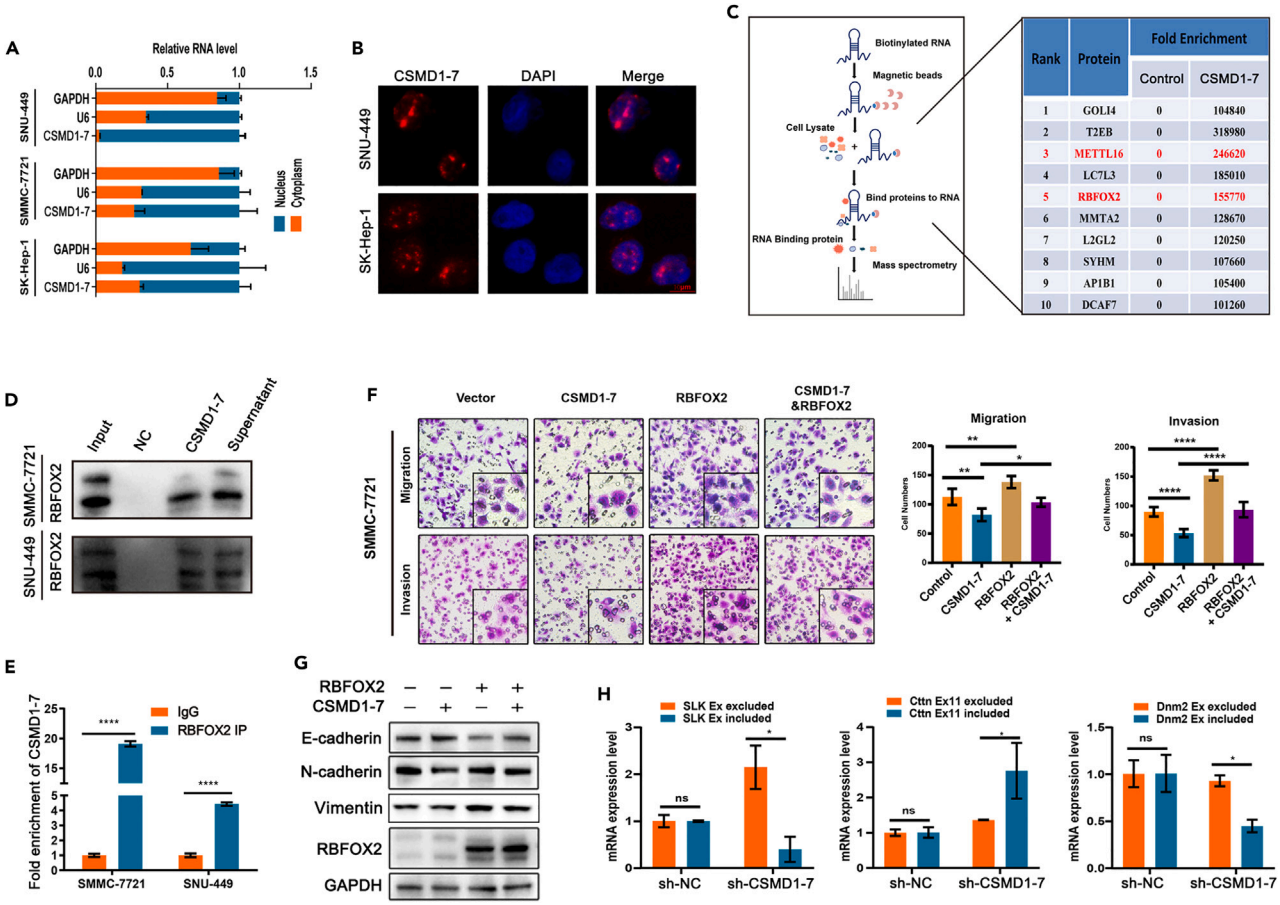

Figure 3. Lnc-CSMD1-7 suppresses EMT by sequestering RBFOX2 protein in HCC

(A) Subcellular fractionation assay confirmed the location of Lnc-CSMD1-7 in SNU-449, SMMC-7721, and SK-Hep-1 cells.

(B) RNA FISH assay show that Lnc-CSMD1-7 was mainly located in the nucleus of HCC cells (SNU-449 and SK-Hep-1 cells). Scale bar: 10 μm.

(C) LncRNA pull-down combined with mass spectrometry to identify Lnc-CSMD1-7 interaction protein (left) and list of potential interacting proteins of Lnc-CSMD1-7 (right).

(D) RNA pull-down assay was performed in SMMC-7721 and SNU449 cells using a biotin-labelled Lnc-CSMD1-7 RNA probe transcribed *in vitro*, and RBFOX2 was detected using Western blots.

(E) RIP-qPCR analysis of the interaction between RBFOX2 and Lnc-CSMD1-7 in SMMC-7721 and SUN449 cells. Enrichment of Lnc-CSMD1-7 with RBFOX2 antibody and IgG control was measured by qPCR.

(F) Representative images and quantification results of transwell cell migration and invasion assay in SMMC-7721 cells stably transfected with Lnc-CSMD1-7, RBFOX2, and co-transfected with Lnc-CSMD1-7 and RBFOX2.

(G) Western blotting analysis of EMT-associated markers in SMMC-7721 and SNU449 cells as indicated.

(H) Alternative splicing of epithelial-specific Rbfox2 targets in Lnc-CSMD1-7-depleted cells. Lnc-CSMD1-7-dependent inclusion of Slk exon 13, Dnm2 12-nt exon, and Cttn exon 11.

Graph data were presented as mean ± SEM. *p < 0.05,**p < 0.01, ****p < 0.0001 (Student's *t* test).

METTL16-mediated m6A modification decreases the stability of Lnc-CSMD1-7

Next, we further investigated the mechanism of downregulation of Lnc-CSMD1-7 expression in HCC. In our previous experimental results in Figure 3C, we also identified another potential interacting protein of Lnc-CSMD1-7, METTL16, which is an m6A methyltransferase. Therefore, we speculate that METTL16 may regulate the expression of Lnc-CSMD1-7 by mediating its m6A modification. To verify our hypothesis, we firstly confirmed the interaction between Lnc-CSMD1-7 and METTL16 using RNA-pull down/western blot (Figure 4A). The interaction between Lnc-CSMD1-7 and METTL16 was also confirmed by RIP/qRT-PCR assay (Figure 4B). To determine whether METTL16 binding to Lnc-CSMD1-7 affected its m6A methylation modification, me-RIP/qRT-PCR assay was performed, and the result showed that METTL16 overexpression significantly increased the m6A modification of Lnc-CSMD1-7 (Figure 4C). Furthermore, METTL16 knockdown dramatically improved the expression of Lnc-CSMD1-7 (Figure 4D). In contrast, the expression of Lnc-CSMD1-7 was inhibited by METTL16 overexpression (Figure 4D). Previous studies have shown that m6A methylation regulates RNA metabolism, including degradation.[18] Therefore, we

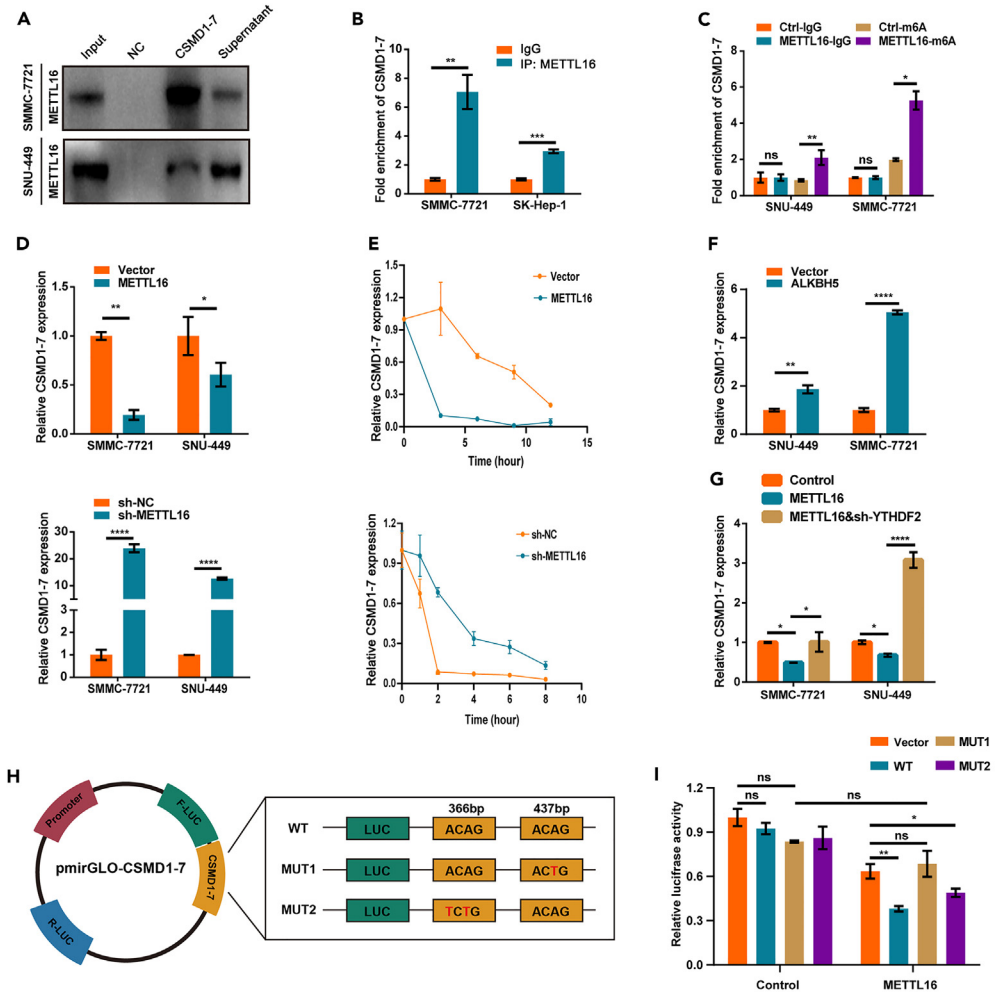

Figure 4. METTL16-mediated m6A modification represses Lnc-CSMD1-7 expression in HCC

(A) RNA pull-down assay was performed in SMMC-7721 and SNU449 cells using a biotin-labelled Lnc-CSMD1-7 RNA probe transcribed *in vitro*, and METTL16 was detected by western blots.

(B) RIP-qPCR analysis of the interaction between METTL16 and Lnc-CSMD1-7 in SMMC-7721 and SK-Hep-1 cells.

(C) meRIP-qPCR analysis was used to detect METTL16-mediated Lnc-CSMD1-7 m6A modification in SNU-449 and SMMC-7721 cells.

(D) The expression of Lnc-CSMD1-7 in METTL16 or shMETTL16 cells was quantified by real-time PCR.

(E) The expression of Lnc-CSMD1-7 in METTL16 or shMETTL16 cells at the indicated time points after actinomycin D treatment and the decay rate of Lnc-CSMD1-7 was evaluated with a linear regression model.

(F) ALKBH5 was overexpressed in SMMC-7721 and SNU449 cells, and the expression of Lnc-CSMD1-7 was detected by qPCR.

(G) METTL16 was overexpressed and YTHDF2 was knocked down in SMMC-7721 and SNU449 cells as indicated, and the expression of Lnc-CSMD1-7 was detected by qPCR.

(H) Wild-type Lnc-CSMD1-7 and Lnc-CSMD1-7 with a mutation at the m6A consensus sequence were cloned into a luciferase reporter.

(I) Relative luciferase activity of the wildtype and mutant Lnc-CSMD1-7 reporter vectors catalyzed by METTL16.

Graph data were presented as mean ± SEM. *p < 0.05,**p < 0.01, ***p < 0.001, ****p < 0.0001 (Student's *t* test).

speculated that METTL16-induced Lnc-CSMD1-7 m6A methylation may downregulate RNA expression by promoting RNA degradation. RNA stability assay showed that METTL16 knockdown increased the stability of Lnc-CSMD1-7 (Figure 4E). Correspondingly, overexpression of METTL16 accelerated the degradation Lnc-CSMD1-7 (Figure 4E).

To further identify the m6A erasers and readers involved in the regulation of Lnc-CSMD1-7 degradation, the m6A demethylase ALKBH5 was overexpressed in SUN-449 and SMMC-7721 cells. As shown in Figure 4F, ALKBH5 significantly upregulated the expression of Lnc-CSMD1-7. In addition, knockdown of the m6A "reader" YTHDF2 significantly inhibited the downregulatory effect of METTL16 on Lnc-CSMD1-7 expression (Figure 4G). Therefore, the aforementioned results indicate that METTL16, ALKBH5, and YTHDF2 are involved in m6A installation, removal, and recognition of Lnc-CSMD1-7, respectively. To further confirm the methylation sites in Lnc-CSMD1-7, the online

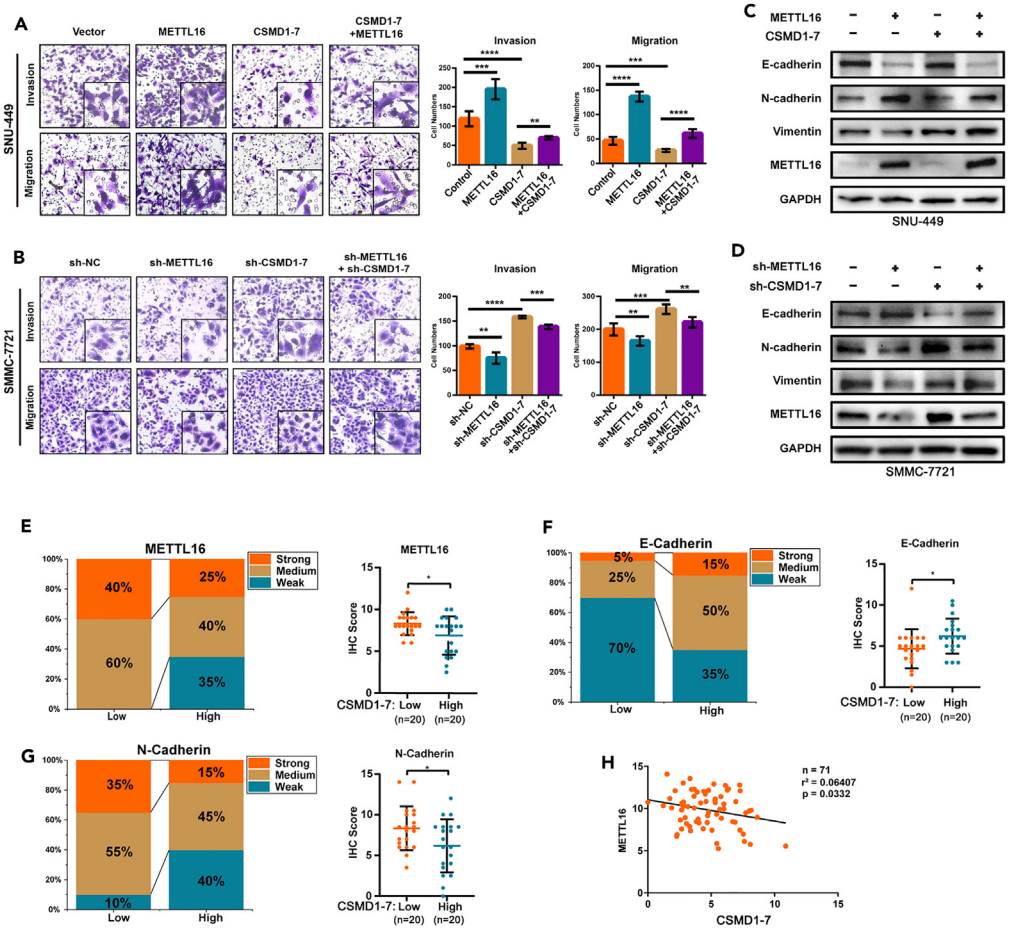

Figure 5. Lnc-CSMD1-7 mediates metastasis-promoting function of METTL16

(A) Representative images and quantification results of transwell cell migration and invasion assay in SNU-449 cells overexpressing METTL16 and Lnc-CSMD1-7.

(B) Representative images and quantification results of transwell cell migration and invasion assay in SMMC-7721 cells with METTL16 and Lnc-CSMD1-7 knockdown.

(C and D) Western blotting detection of EMT-associated markers in SNU-449 (C) and SMMC-7721 (D) cells as indicated.

(E–G) Immunohistochemical staining intensity and IHC score statistics of METT16 (E), E-cadherin (F), and N-cadherin (G) in HCC tissue samples with high and low expression of Lnc-CSMD1-7.

(H) The correlation between METTL16 and Lnc-CSMD1-7 in 71 HCC tissues, the expression of METTL16 and Lnc-CSMD1-7 was detected by qPCR.

Graph data were presented as mean ± SEM. *p < 0.05,**p < 0.01, ***p < 0.001, ****p < 0.0001 (Student's *t* test).

prediction tool SRAMP revealed that numerous m6A sites with high confidence are distributed in Lnc-CSMD1-7 sequence. We then constructed three mutant Lnc-CSMD1-7 3'UTR plasmids for the luciferase reporter assay to determine the specific modification sites (Figure 4H). As shown in Figure 4I, compared with the wild-type Lnc-CSMD1-7, MUT1 reversed the downregulation of luciferase activity caused by METTL16, whereas MUT2 did not affect the luciferase activity, indicating that METTL16 modulated Lnc-CSMD1-7 expression mainly through the MUT1 site but not the MUT2 sites. These results demonstrate that m6A maintains the mRNA stability of Lnc-CSMD1-7 by METTL16 in HCC.

Lnc-CSMD1-7 mediates metastasis-promoting function of METTL16

We next investigated whether METTL16 plays a role in promoting HCC metastasis through negative regulation of Lnc-CSMD1-7. The transwell invasion and migration assays show that METTL16 overexpression can significantly promote the invasion and migration of SNU-449 cells. Furthermore, the inhibition of Lnc-CSMD1-7 on invasion and migration of HCC cells could be reversed by METTL16 (Figures 5A and S3). Similarly, METTL16 knockdown also attenuated the promoting effect of sh-Lnc-CSMD1-7 on HCC cell invasion and migration (Figures 5B and S3). We also detected the expression of E-cadherin, N-cadherin, and vimentin by western blot, and the results showed that METTL16 could reverse the regulation of Lnc-CSMD1-7 on the expression of these EMT-related proteins (Figure 5C). The same phenomenon was observed

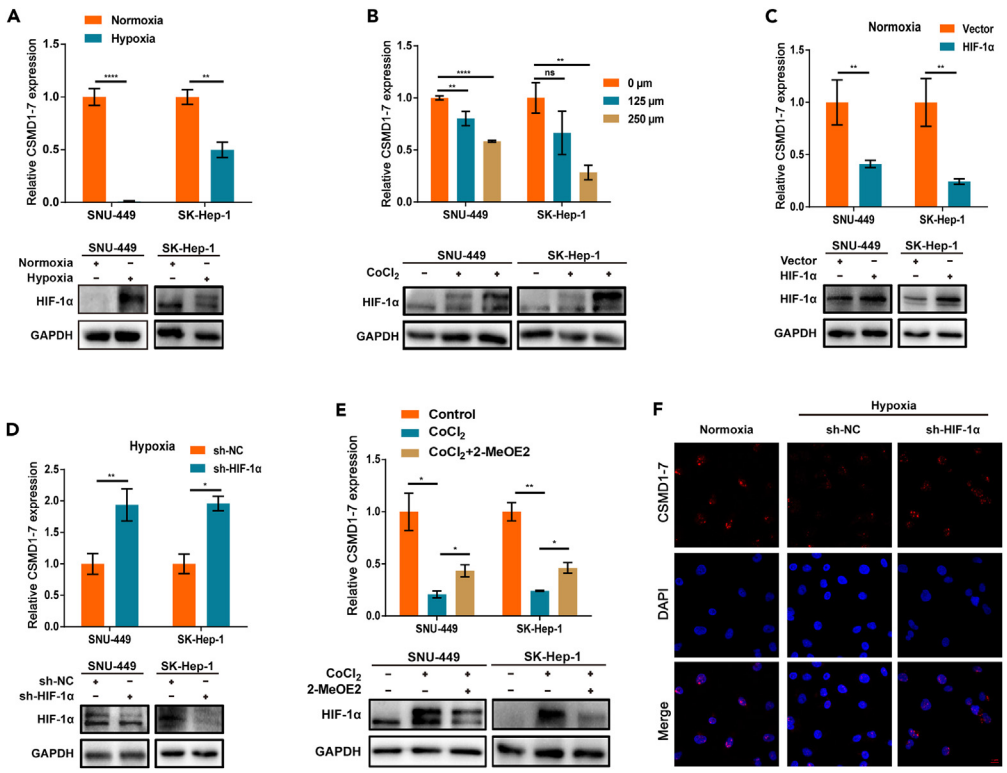

Figure 6. Hypoxia downregulated Lnc-CSMD1-7 expression via HIF-1α

(A) SNU-449 and SK-Hep-1 were cultured under normoxia (20% O_2) or hypoxia (2% O_2), expression of Lnc-CSMD1-7 was detected by qRT-PCR and HIF-1α was detected by western blotting.

(B) SNU-449 and SK-Hep-1 cells were cultured under different concentrations $CoCl_2$, the expression of Lnc-CSMD1-7 was detected by qRT-PCR and HIF-1α was detected using western blotting.

(C) SNU-449 and SK-Hep-1 cells overexpressing HIF-1α or not were cultured under normoxia (20% O_2), and expression of Lnc-CSMD1-7 was detected by qRT-PCR and HIF-1α was detected by western blotting.

(D) SNU-449 and SK-Hep-1 cells with HIF-1α knockdown (sh-HIF-1α) or not (sh-NC) were cultured under hypoxia (2% O_2) and expression of Lnc-CSMD1-7 was detected by qRT-PCR and HIF-1α was detected by western blotting.

(E) SNU-449 and SK-Hep-1 were cultured under $CoCl_2$ or $CoCl_2$+2-MeOE2, expression of Lnc-CSMD1-7 was detected by qRT-PCR and HIF-1α was detected by western blotting.

(F) FISH assay of Lnc-CSMD1-7 in normoxia or hypoxia HCC cells with HIF-1α knockdown (sh-HIF-1α) or not (sh-NC).

Scale bar: 10 μm. Graph data were presented as mean ± SEM. *p < 0.05,**p < 0.01, ***p < 0.001 (Student's *t* test).

in HCC cells with simultaneous METT16 and Lnc-CSMD1-7 knockdown (Figure 5D). These data suggest that METTL16 can promote the invasion and migration of HCC cells through Lnc-CSMD1-7.

Next, we further verified the association of Lnc-CSMD1-7 with METTL16 and HCC metastatic potential in clinical samples. Forty HCC tissue samples were selected for immunohistochemical staining of METTL16, E-cadherin, and N-cadherin, and immunostaining scores were performed according to staining intensity (Figure S4). Our results showed that METTL16 and N-cadherin expression were relatively low, whereas E-cadherin expression was relatively high in HCC tissues with high expression of Lnc-CSMD1-7 (Figures 5E–5G). In addition, METTL16 RNA expression also showed a significant negative correlation with Lnc-CSMD1-7 (Figure 5H). Furthermore, using *in vivo* experiments in mice, we also observed that overexpressing METTL16 promoted lung metastasis of HCC (Figure S5). In conclusion, METTL16 promotes HCC metastasis via Lnc-CSMD1-7.

Hypoxia downregulated Lnc-CSMD1-7 expression via HIF-1α

Hypoxia is a common phenomenon in HCC and can trigger a series of pro-metastatic molecular events in HCC and worsen the prognosis.[19] Recent studies, including our previous study, have shown that the aberrant expression of some lncRNAs is attributed to the hypoxic microenvironment of cancers.[20,21] We wondered whether the decreased expression of Lnc-CSMD1-7 in HCC is regulated by hypoxia. After treatment with hypoxia for 24 h, the expression of Lnc-CSMD1-7 in SNU-449 and SK-Hep-1 cells was apparently reduced along with the increase in HIF-1α expression (Figure 6A). Treatment with $CoCl_2$, a chemical inducer of hypoxia, also decreased the expression of Lnc-CSMD1-7 in a dose-dependent manner (Figure 6B). In addition, overexpression of HIF-1α significantly inhibited the expression of Lnc-CSMD1-7 (Figure 6C).

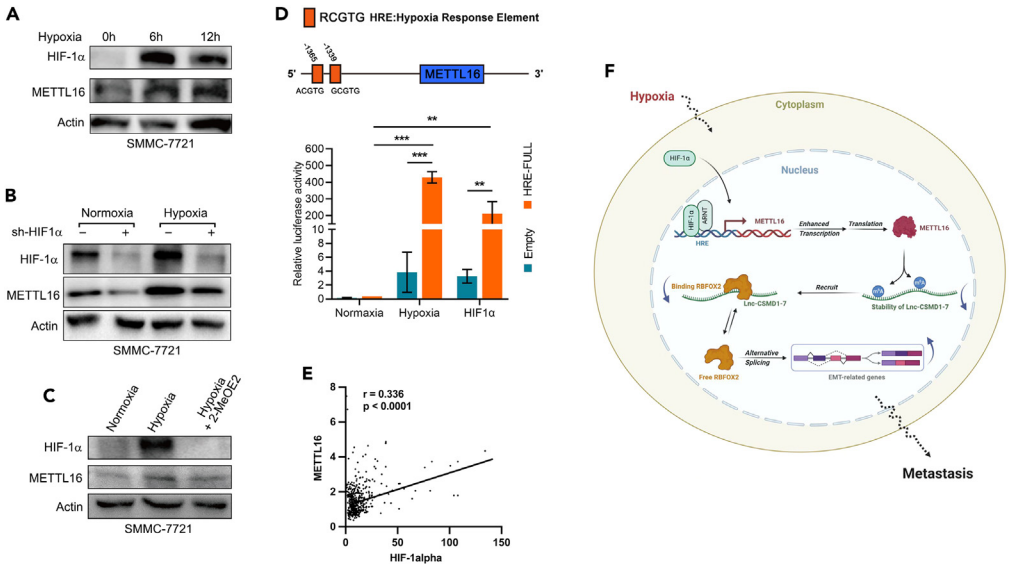

Figure 7. Hypoxia induces HCC metastasis via the HIF-1α/METTL16/Lnc-CSMD1-7/RBFOX2 axis

(A) Western blot analysis of METTL16 and HIF-1αin SMMC-7721 cells at indicated time points after culture under hypoxia (2% O_2).

(B) SMMC-7721 cells with or without HIF-1α knockdown were cultured under normoxia (20% O_2) or hypoxia (2% O_2), the expression of METTL16 and HIF-1α was detected by western blot.

(C) SMMC-7721 cells were cultured under normoxia (20% O_2) or hypoxia (2% O_2) and treated with 2-MeOE2, the expression of METTL16 and HIF-1α was detected by western blot.

(D) The schematic illustration of HRE regions in METTL16 promoter; luciferase reporter gene assays were performed to compare the luciferase activity of the full-length METTL16 promoter under normal oxygen or hypoxic conditions.

(E) The correlation between HIF-1α mRNA level and METTL16 level in TCGA datasets.

(F) Schematic overview of hypoxia induces hepatocellular carcinoma metastasis via the HIF-1α/METTL16/Lnc-CSMD1-7/RBFOX2 axis.

On the contrary, HIF-1α knockdown dramatically promotes Lnc-CSMD1-7 expression under hypoxia condition (Figures 6D and 6F). Furthermore, the $CoCl_2$-induced downregulation of Lnc-CSMD1-7 could be inhibited by the HIF-1α inhibitor 2-MeOE2 (Figure 6E). Therefore, the aforementioned data suggest that hypoxia downregulates Lnc-CSMD1-7 expression via HIF-1α.

Hypoxia induces HCC metastasis via the HIF-1α/METTL16/Lnc-CSMD1-7/RBFOX2 axis

Hypoxia is known to promote tumorigenesis, angiogenesis and metastasis, and also modulates the levels of m6A writer, eraser, and reader, which, in turn, regulate hypoxic conditions and enhance adaptation to hypoxia.[22] For example, HIF-1α-induced YTHDF1 expression was associated with hypoxia-induced autophagy and autophagy-related HCC progression via promoting translation of autophagy-related genes ATG2A and ATG14 in an m6A-dependent manner.[23] Therefore, we hypothesized that METTL16-induced methylation mediated the negative regulation of Lnc-CSMD1-7 by hypoxia. To test this hypothesis, we first determined whether hypoxia regulates METTL16 expression. As we expected, hypoxia upregulated METTL16 expression (Figure 7A), whereas knockdown of HIF-1α significantly downregulated METTL16 expression (Figure 7B). In addition, the regulation of METTL16 expression by hypoxia was also inhibited by treatment with the HIF-1α inhibitor 2-MeOE2 (Figure 7C), suggested that hypoxia-induced upregulation of METTL16 depends on HIF-1α. It is well known that HIF-1α binds to an identical core-binding motif also known as the HRE (5′-RCGTG-3′) and commonly upregulated certain gene expression.[24] Therefore, we analyzed the sequence of the promoter region of METTL16 and found two potential HREs (Figure 7D). Subsequent luciferase reporter experiments confirmed that HIF-1α could bind to the HRE in the promoter region of METTL16 and transcriptionally upregulate the expression of METTL16 (Figure 7D). In addition, we analyzed the expression of METTL16 and HIF-1α in the TCGA database, and the results showed a significant positive correlation between them (Figure 7E).

Taken together, we propose that the hypoxic microenvironment in HCC upregulates the expression of METTL16 through HIF-1α, and METTL16 binds to Lnc-CSMD1-7 and promotes the degradation of Lnc-CSMD1-7 via m6A methylation modification. Thus, hypoxia contributes to reduce the levels of Lnc-CSMD1-7 in HCC. In addition, Lnc-CSMD1-7 directly binds to the RNA splicing factor RBFOX2, inhibiting Rbfox2-regulated splicing shifts from epithelial to mesenchymal-specific events, thereby inhibiting EMT and metastasis of HCC. Finally, Hypoxia promoted HCC metastasis through the HIF-1α/METTL16/Lnc-CSMD1-7/RBFOX2 axis (Figure 7F).

DISCUSSION

Hypoxia is observed in almost every solid tumor including HCC, and it has even been considered as a therapeutic target for HCC.[4] Within the tumor microenvironment, hypoxia is a potent metastasis-promoting factor. Clinically, hypoxia and HIF expression are associated with

increased distant metastasis and poor survival in a variety of tumors.[2,25] To date, the mechanisms by which the hypoxic tumor microenvironment promotes metastatic progression are not fully understood. In our study, the hypoxic microenvironment upregulated the expression of METTL16 via HIF-1α, and METTL16 was able to directly bind to Lnc-CSMD1-7 and promote its m6A methylation modification, thereby promoting the degradation of Lnc-CSMD1-7, which leads to the downregulation of Lnc-CSMD1-7 in HCC. In addition, our study also found that Lnc-CSMD1-7 can directly bind to RBFOX2, affect its function on alternative splicing of EMT-related genes, and inhibit the metastasis of HCC. Finally, our study demonstrated that the hypoxic microenvironment promotes HCC metastasis through the HIF-1α/METTL16/Lnc-CSMD1-7/RBFOX2 axis.

Previous studies have reported the involvement of ncRNA in alternative splicing.[26] LncRNA NEAT1 was reported to regulate the phosphorylation status of splicing factor SRp40 and regulate alternative splicing of PPARγ mRNA.[27] circRAPGEF5 can bind to the Fox-1 C-terminal domain of RBFOX2 and induce specific exon exclusion of TFRC by preventing RBFOX2 binding to pre-mRNA.[16] A recent investigation revealed that circURI1 interacts with hnRNPM to inhibit metastasis by modulating the AS of VEGFA in gastric cancer.[28] In our study, Lnc-CSMD1-7 also directly binds to RBFOX2 and affects alternative splicing of Slk, Cttn, and Dnm2 mRNA. However, whether Lnc-CSMD1-7 regulates AS by obstructing the binding of RBFOX2 to pre-mRNA remains to be elucidated.

METTL16 is a recently identified m6A methyltransferase. Compared to other m6A regulatory proteins, very few m6A-modified substrates regulated by METTL16 have been discovered so far. METTL16 is upregulated in a variety of tumors, including glioma,[29] melanoma,[30] HCC,[10] and gastric cancer.[31] However, the mechanism of upregulation of METTL16 expression in tumors is still lacking. In our study, the upregulation of METTL16 induced by hypoxic microenvironment was reported for the first time. Furthermore, the involvement of METTL16 in cancer is largely unknown. METTL16 promotes HCC progression by downregulating RAB11B-AS1 in an m6A-dependent manner.[10] METTL16 promotes cell proliferation by upregulating cyclin D1 expression in gastric cancer.[31] In our work, METTL16 promotes HCC metastasis by promoting the degradation of Lnc-CSMD1-7 in an m6A-dependent manner. These results not only extend the understanding of METTL16-modified substrates but also provide evidence for the effects of m6A modification on RNA stability.

In summary, we show that hypoxia transcriptionally upregulates the expression of METTL16 via HIF-1α and METTL16-mediated m6A modification reduces the stability of Lnc-CSMD1-7. Lnc-CSMD1-7 directly binds to the RBFOX2, thereby affecting RBFOX2-regulated alternative splicing in EMT related genes, and then negatively regulate the invasion and migration of HCC cells. Taken together, we demonstrate that the HIF-1α/METTL16/Lnc-CSMD1-7/RBFOX2 axis mediates hypoxia-induced HCC metastasis.

Limitations of the study

Out study explores the molecular mechanism by which Lnc-CSMD1-7 regulates the progression of hepatocellular carcinoma through its binding to RBFOX2. However, further studies are required to identify the specific domain of the interaction between lnc-CSMD1-7 and RBFOX2, and to determine how Lnc-CSMD1-7 affects the variable splicing of its downstream target genes by RBFOX2. On the other hand, METTL16, as an m6A methyltransferase, has the ability to methylate a variety of RNA substrates. Our study demonstrates that the METTL16/Lnc-CSMD1-7/RBFOX2 signaling pathway facilitates hypoxia-induced HCC metastasis. However, Lnc-CSMD1-7 is merely one of the methylation targets of METT16; the latter is probably involved in regulating tumor progression via other downstream genes. Thus, it is imperative to further investigate the role of METTL16 in tumor progression.

STAR★METHODS

Detailed methods are provided in the online version of this paper and include the following:

- KEY RESOURCES TABLE
- RESOURCE AVAILABILITY
  - Lead contact
  - Materials availability
  - Data and code availability
- EXPERIMENTAL MODEL AND STUDY PARTICIPANT DETAILS
  - Ethics approval and consent to participate
  - Patients and tissue specimens
  - Cell lines
  - Mice
- METHOD DETAILS
  - Total RNA extraction and real-time quantitative PCR
  - Cell transfection
  - Subcellular fractionation analysis
  - Cell invasion, migration and scratch-wound healing assay
  - Western Blot
  - RNA pull-down assay
  - RNA fluorescence *in situ* hybridization (RNA-FISH)

- RNA immunoprecipitation (RIP) assays
- Dual-luciferase reporter assays

- QUANTIFICATION AND STATISTICAL ANALYSIS

SUPPLEMENTAL INFORMATION

Supplemental information can be found online at https://doi.org/10.1016/j.isci.2023.108495.

ACKNOWLEDGMENTS

This work was supported by Science and Technology Projects of Fujian Province (2019Y9047, 2021Y9032, 2022L3030, 2020J011164, 2020J011156), Fujian Provincial Health Technology Project (2021ZQNZD014, 2020GGA072), Scientific Foundation of Fuzhou Municipal Health commission (2021-S-wt2, 2021-S-wt3, 2021-S-wt4, 2021-S-wp1).

AUTHOR CONTRIBUTIONS

Y.W., B.Z., X.L., and W.G. conceptualized the study; Y.W., Yo.Y., Ye.Y., Z.G. performed experiments; Y. W., Y.D., Q. Z., X.Z., F.W., N.C., B.Z., and W.G. performed statistical analysis; B.Z. and X.L. prepared the manuscript.

DECLARATION OF INTERESTS

The authors declare no competing interests.

Received: June 27, 2023
Revised: October 6, 2023
Accepted: November 16, 2023
Published: November 19, 2023

REFERENCES

1. Sung, H., Ferlay, J., Siegel, R.L., Laversanne, M., Soerjomataram, I., Jemal, A., and Bray, F. (2021). Global Cancer Statistics 2020: GLOBOCAN Estimates of Incidence and Mortality Worldwide for 36 Cancers in 185 Countries. CA. Cancer J. Clin. *71*, 209–249.
2. Rankin, E.B., and Giaccia, A.J. (2016). Hypoxic control of metastasis. Science *352*, 175–180.
3. Harris, A.L. (2002). Hypoxia–a key regulatory factor in tumour growth. Nat. Rev. Cancer *2*, 38–47.
4. Wu, X.Z., Xie, G.R., and Chen, D. (2007). Hypoxia and hepatocellular carcinoma: The therapeutic target for hepatocellular carcinoma. J. Gastroenterol. Hepatol. *22*, 1178–1182.
5. Peng, L., Yuan, X.Q., Zhang, C.Y., Peng, J.Y., Zhang, Y.Q., Pan, X., and Li, G.C. (2018). The emergence of long non-coding RNAs in hepatocellular carcinoma: an update. J. Cancer *9*, 2549–2558.
6. Yang, F., Huo, X.S., Yuan, S.X., Zhang, L., Zhou, W.P., Wang, F., and Sun, S.H. (2013). Repression of the long noncoding RNA-LET by histone deacetylase 3 contributes to hypoxia-mediated metastasis. Mol. Cell *49*, 1083–1096.
7. Shao, M., Yang, Q., Zhu, W., Jin, H., Wang, J., Song, J., Kong, Y., and Lv, X. (2018). LncHOXA10 drives liver TICs self-renewal and tumorigenesis via HOXA10 transcription activation. Mol. Cancer *17*, 173.
8. Huang, H., Weng, H., and Chen, J. (2020). m(6)A Modification in Coding and Non-coding RNAs: Roles and Therapeutic Implications in Cancer. Cancer Cell *37*, 270–288.
9. Han, L., Dong, L., Leung, K., Zhao, Z., Li, Y., Gao, L., Chen, Z., Xue, J., Qing, Y., Li, W., et al. (2023). METTL16 drives leukemogenesis and leukemia stem cell self-renewal by reprogramming BCAA metabolism. Cell Stem Cell *30*, 52–68.e13.
10. Dai, Y.Z., Liu, Y.D., Li, J., Chen, M.T., Huang, M., Wang, F., Yang, Q.S., Yuan, J.H., and Sun, S.H. (2022). METTL16 promotes hepatocellular carcinoma progression through downregulating RAB11B-AS1 in an m(6)A-dependent manner. Cell. Mol. Biol. Lett. *27*, 41.
11. Ule, J., and Blencowe, B.J. (2019). Alternative Splicing Regulatory Networks: Functions, Mechanisms, and Evolution. Mol. Cell *76*, 329–345.
12. Roy Burman, D., Das, S., Das, C., and Bhattacharya, R. (2021). Alternative splicing modulates cancer aggressiveness: role in EMT/metastasis and chemoresistance. Mol. Biol. Rep. *48*, 897–914.
13. Braeutigam, C., Rago, L., Rolke, A., Waldmeier, L., Christofori, G., and Winter, J. (2014). The RNA-binding protein Rbfox2: an essential regulator of EMT-driven alternative splicing and a mediator of cellular invasion. Oncogene *33*, 1082–1092.
14. Venables, J.P., Brosseau, J.P., Gadea, G., Klinck, R., Prinos, P., Beaulieu, J.F., Lapointe, E., Durand, M., Thibault, P., Tremblay, K., et al. (2013). RBFOX2 is an important regulator of mesenchymal tissue-specific splicing in both normal and cancer tissues. Mol. Cell Biol. *33*, 396–405.
15. Jbara, A., Lin, K.T., Stossel, C., Siegfried, Z., Shqerat, H., Amar-Schwartz, A., Elyada, E., Mogilevsky, M., Raitses-Gurevich, M., Johnson, J.L., et al. (2023). RBFOX2 modulates a metastatic signature of alternative splicing in pancreatic cancer. Nature *617*, 147–153.
16. Zhang, J., Chen, S., Wei, S., Cheng, S., Shi, R., Zhao, R., Zhang, W., Zhang, Q., Hua, T., Feng, D., et al. (2022). CircRAPGEF5 interacts with RBFOX2 to confer ferroptosis resistance by modulating alternative splicing of TFRC in endometrial cancer. Redox Biol. *57*, 102493.
17. Geisler, S., and Coller, J. (2013). RNA in unexpected places: long non-coding RNA functions in diverse cellular contexts. Nat. Rev. Mol. Cell Biol. *14*, 699–712.
18. He, L., Li, H., Wu, A., Peng, Y., Shu, G., and Yin, G. (2019). Functions of N6-methyladenosine and its role in cancer. Mol. Cancer *18*, 176.
19. Wong, C.C.L., Kai, A.K.L., and Ng, I.O.L. (2014). The impact of hypoxia in hepatocellular carcinoma metastasis. Front. Med. *8*, 33–41.
20. Zhao, B., Ke, K., Wang, Y., Wang, F., Shi, Y., Zheng, X., Yang, X., Liu, X., and Liu, J. (2020). HIF-1alpha and HDAC1 mediated regulation of FAM99A-miR92a signaling contributes to hypoxia induced HCC metastasis. Signal Transduct. Targeted Ther. *5*, 118.
21. Deng, S.J., Chen, H.Y., Ye, Z., Deng, S.C., Zhu, S., Zeng, Z., He, C., Liu, M.L., Huang, K., Zhong, J.X., et al. (2018). Hypoxia-induced LncRNA-BX111 promotes metastasis and progression of pancreatic cancer through regulating ZEB1 transcription. Oncogene *37*, 5811–5828.
22. Gu, Y., Wu, X., Zhang, J., Fang, Y., Pan, Y., Shu, Y., and Ma, P. (2021). The evolving landscape of N(6)-methyladenosine modification in the tumor microenvironment. Mol. Ther. *29*, 1703–1715.
23. Li, Q., Ni, Y., Zhang, L., Jiang, R., Xu, J., Yang, H., Hu, Y., Qiu, J., Pu, L., Tang, J., and Wang, X. (2021). HIF-1alpha-induced expression of m6A reader YTHDF1 drives hypoxia-induced autophagy and malignancy of hepatocellular carcinoma by promoting ATG2A and ATG14 translation. Signal Transduct. Targeted Ther. *6*, 76.

24. Lee, J.W., Ko, J., Ju, C., and Eltzschig, H.K. (2019). Hypoxia signaling in human diseases and therapeutic targets. Exp. Mol. Med. *51*, 1–13.
25. Rankin, E.B., and Giaccia, A.J. (2008). The role of hypoxia-inducible factors in tumorigenesis. Cell Death Differ. *15*, 678–685.
26. Liu, Y., Liu, X., Lin, C., Jia, X., Zhu, H., Song, J., and Zhang, Y. (2021). Noncoding RNAs regulate alternative splicing in Cancer. J. Exp. Clin. Cancer Res. *40*, 11.
27. Cooper, D.R., Carter, G., Li, P., Patel, R., Watson, J.E., and Patel, N.A. (2014). Long Non-Coding RNA NEAT1 Associates with SRp40 to Temporally Regulate PPARgamma2 Splicing during Adipogenesis in 3T3-L1 Cells. Genes *5*, 1050–1063.
28. Wang, X., Li, J., Bian, X., Wu, C., Hua, J., Chang, S., Yu, T., Li, H., Li, Y., Hu, S., et al. (2021). CircURI1 interacts with hnRNPM to inhibit metastasis by modulating alternative splicing in gastric cancer. Proc. Natl. Acad. Sci. USA *118*, e2012881118.
29. Cong, P., Wu, T., Huang, X., Liang, H., Gao, X., Tian, L., Li, W., Chen, A., Wan, H., He, M., et al. (2021). Identification of the Role and Clinical Prognostic Value of Target Genes of m6A RNA Methylation Regulators in Glioma. Front. Cell Dev. Biol. *9*, 709022.
30. Liu, J., Zhou, Z., Ma, L., Li, C., Lin, Y., Yu, T., Wei, J.F., Zhu, L., and Yao, G. (2021). Effects of RNA methylation N6-methyladenosine regulators on malignant progression and prognosis of melanoma. Cancer Cell Int. *21*, 453.
31. Wang, X.K., Zhang, Y.W., Wang, C.M., Li, B., Zhang, T.Z., Zhou, W.J., Cheng, L.J., Huo, M.Y., Zhang, C.H., and He, Y.L. (2021). METTL16 promotes cell proliferation by up-regulating cyclin D1 expression in gastric cancer. J. Cell Mol. Med. *25*, 6602–6617.

STAR★METHODS

KEY RESOURCES TABLE

REAGENT or RESOURCE	SOURCE	IDENTIFIER
Antibodies		
Anti-E-Cadherin	Cell Signaling Technology	Cat# 3195; RRID: AB_2291471
Anti-N-Cadherin	Cell Signaling Technology	Cat# 13116; RRID: AB_2687616
Anti-vimentin	Cell Signaling Technology	Cat# 5741s; RRID: AB_10695459
Anti-METTL16	Abcam	Cat# ab313743; RRID: AB_3075502
Anti- FOX2/RBM9	Proteintech	Cat# 12498; RRID: AB_2877861
Anti-HIF-1α	Santa Cruz	Cat# sc53546; RRID: AB_629639
Anti-GAPDH	Cell Signaling Technology	Cat# 5174; RRID: AB_10622025
Anti-β-Actin	Cell Signaling Technology	Cat# 12262; RRID: AB_2566811
Biological samples		
Omental adipose tissue	Mengchao Hepatobiliary Hospital of Fujian Medical University	N/A
Chemicals, peptides, and recombinant proteins		
$CoCl_2$	Sigma-Aldrich	449776
2-MeOE2	Selleck	S1233
Critical commercial assays		
TransZol Up Plus RNA Kit	transgen	ER501-01-V2
Hifair® II 1st Strand cDNA Synthesis Kit(gDNA digester plus)	yeasen	11121ES60
SYBR Green qPCR Mix	DBI	DBI-2043
Magna RIP™	merck	17–700
EZ-ChIP™	millipore	17–371
RNA 3′ End Biotinylation Kit	thermofisher	20160
RNeasy Mini Kit	Qiagen	74104
T7 High Yield RNA Transcription Kit	vazyme	TR101-01
Mut Express II Fast Mutagenesis Kit V2	vazyme	C214-01
Lipofectamine™ 3000 Transfection Reagent	thermofisher	L3000015
TransDetect® Double-Luciferase Reporter Assay Kit	transgen	FR201
Experimental models: Cell lines		
SK-Hep-1	American Type Culture Collection	N/A
SNU-449	American Type Culture Collection	N/A
HEK-293T	American Type Culture Collection	N/A
SMMC-7721	Chinese Academy of Sciences	N/A
Experimental models: Organisms		
B-NSG mice	Biocytogen	N/A
Oligonucleotides		
See Tables S1 and S2	Sangon Biotech	N/A
Software and algorithms		
SPSS 25.0	IBM SPSS	N/A
GraphPad Prism 6.0	GraphPad	N/A

RESOURCE AVAILABILITY

Lead contact

Further information and requests for resources and reagents should be directed to and will be fulfilled by the lead contact, Bixing Zhao (e-mail: bixingzhao@gmail.com).

Materials availability

The plasmids and cell lines generated in this study are available from the lead contact upon request.

Data and code availability

- Data reported in this paper will be shared by the lead contact upon request.
- This paper does not report original code.
- Any additional information required to reanalyze the data reported in this paper is available from the lead contact upon request.

EXPERIMENTAL MODEL AND STUDY PARTICIPANT DETAILS

Ethics approval and consent to participate

All enrolled patients provided written informed consent and this study was approved by the ethics committee of Mengchao Hepatobiliary Hospital of Fujian Medical University. All animal experiments were approved by the Experimental Animal Ethics Committee of Mengchao Hepatobiliary Hospital, Fujian Medical University.

Patients and tissue specimens

For RNA-seq assay, 61 freshly frozen HCC tumor and their paired adjacent non-tumor tissues were obtained from the bio-bank of Mengchao Hepatobiliary Hospital of Fujian Medical University. For validation and prognosis analysis, another sample cohort including HCC tumor and nontumor tissues were collected from 97 HCC patients aged 30–75 years, with no restriction on gender, ancestry, race or ethnicity or socio-economic information, with clinical characteristics and long-term follow-up data at Mengchao Hepatobiliary Hospital of Fujian Medical University from January 2016 to December 2020, none of whom had received radiotherapy or chemotherapy, and no other cancer co-morbidities. During surgery, tumor tissues and paracancerous tissues were collected, immediately placed in liquid nitrogen, and then transferred to a refrigerator at −80°C for storage. All enrolled patients gave informed consent before this study, and the study was approval by the Medical Ethics Committee of Mengchao Hepatobiliary Hospital of Fujian Medical University.

Cell lines

Human HCC cell lines SNU-449, SK-Hep-1 and human embryonic kidney cell HEK-293T were obtained from the American Type Culture Collection (ATCC). The SMMC-7721 cell line was obtained from the Chinese Academy of Sciences. The SNU-449 cell line was cultured in RPMI 1640 medium (Gibco) with 10% fetal bovine serum (FBS) while other cell lines were cultured in Dulbecco's modified Eagle's medium (DMEM, Gibco). All cells were cultured in a 5% CO_2 incubator at 37°C. To induce cellular hypoxia, cells were exposed to 2% O_2, 5% CO_2, 93% N_2 through a hypoxia incubation chamber (Billups rothenberg) or treated with different concentrations of cobalt chloride ($CoCl_2$, Sigma-Aldrich) for 24 h.

Mice

All female B-NSG mice (4 weeks old) were purchased from Biocytogen (Beijing, China) and fed under standard conditions (temperature, 25°C; humidity, 40–60%; 12-h light/dark cycle; free access to standard sterile food and water) in a pathogen-free environment. Protocol used for animal experiments was approved by the Experimental Animal Ethics Committee of Mengchao Hepatobiliary Hospital, Fujian Medical University. 1×10^6 stably transfected SMMC-7721 and SK-Hep-1 cells were injected into mice via the tail vein. After 4–8 weeks, the mice were sacrificed, the lungs were removed and photographed using a multifunctional imager (BIO-RAD). Then, parts of tumor tissues were embedded in paraffin for H&E and immunohistochemistry (IHC) staining.

METHOD DETAILS

Total RNA extraction and real-time quantitative PCR

Total RNA was extracted from clinical HCC samples and cultured HCC cells using TransZol Up RNA kit (TransGen), and the quality and concentration of RNA was measured using NanoDropND-2000 (Thermo Scientific). 1 μg total RNA was reverse transcribed using Hifair 1st strand cDNA synthesis kit (YEASEN) according to the manufacturer's instructions. RT-qPCR was then performed using the Bsetar SYBR Green qPCR Mastermix (DBI) and a StepOne Plus real-time PCR system (Applied Biosystems). Relative gene expression was determined by $2^{-\Delta\Delta Ct}$ and RT-qPCR data were normalized to the 18s rRNA values. The primers for RNA were shown in key resources table

Cell transfection

Cells were seeded in 6-well paltes and cultured at 37°C in 5% CO_2 overnight. Then, the cells were transfected with plasmids using Lipofectamine 3000 Reagent (Thermo Scientific) according to the manufacturer's instructions. Cells were collected after 48 h. The sequences are provided in key resources table.

Subcellular fractionation analysis

Subcellular isolation of the nuclear and cytosolic RNA was performed using NE-PER Nuclear and Cytoplasmic Extraction Reagents (Thermo Scientific) according to the manufacturer's instructions. For quantification of Lnc-CSMD1-7, U6 and GAPDH were used as nuclear and cytoplasmic positive controls respectively.

Cell invasion, migration and scratch-wound healing assay

Cell invasion and migration assays were performed using a Transwell chamber (Corning-Costar). Briefly, SMMC-7721 and SNU-449 cells were resuspended in 200 μL serum-free medium and seeded into an upper Transwell chamber, while 600 μL medium containing 10% FBS was added to the lower chamber. The invasion assay was performed in the same protocol as the migration experiments expect for with Matrigel (Corning-Costar) hydrated in the upper chamber for at least 4 h before cell addition. The cells were then cultured at 37°C for 12–24 h. For the scratch-wound healing assay, cells were seeded in a Culture-Insert (ibidi), after overnight incubation, the insert and original medium were removed, and fresh serum-free or low serum medium was added. The wound was photographed under a microscope at various times.

Western Blot

HCC cells were harvested and lysed with RIPA buffer (Beyotime Biotechnology, China) supplemented with cocktail protease inhibitors and PMSF. Equal amounts of protein lysates were separated by SDS-PAGE and transferred to nitrocellulose membrane. The membranes were probed with the following primary antibodies: E-cadherin (#3195, Cell Signaling Technology, USA), N-cadherin (#13116, Cell Signaling Technology, USA), Vimentin(#5741S, Cell Signaling Technology, USA), HIF1-α (sc-53546, Santa Cruz, USA), FOX2/RBM9 (#12498, Proteintech), METTL16 (#ab313743, Abcam, MA, USA), respectively. GAPDH (#5174, Cell Signaling Technology, USA) or β-Actin (ab6277, abcam) was used as the loading control for normalization.

RNA pull-down assay

RNA pull-down assay was performed using a Pierce Magnetic RNA-Protein Pull-Down Kit (Thermo Scientific) according to the manufacturer's instructions. Briefly, full-length Lnc-CSMD1-7 was amplified with primers containing the T7 promoter sequence and transcribed *in vitro* using T7 High Yield RNA Transcription Kit (Vazyme). RNA was immediately purified using the RNeasy Mini Kit (QIAGEN) and biotin labeled using the Pierce RNA 3′ End Biotinylation Kit (Thermo Scientific). The labeled RNA probes were then bound to streptavidin magnetic beads in RNA capture buffer for 30 min at room temperature with agitation. The beads were collected by a magnetic stand and incubated with cell lysates overnight at 4°C. After washing and elution of RNA-binding protein complexes, proteins were detected by Western blot and mass spectrometry.

RNA fluorescence *in situ* hybridization (RNA-FISH)

SNU-449 and SK-Hep-1 cells were seeded on the slides in 24-well plates. All cells were then fixed and permeabilized with 4% paraformaldehyde (Servicebio) containing 0.5% Triton-100 for 30 min at room temperature. After washing with PBS, the cells were incubated with pre-hybridization solution for 30 min at 37°C and then incubated in hybridization buffer containing DIG-labelled Lnc-CSMD1-7 probe (Servicebio) at 37°C overnight. After washing with SSC solution, the cells were incubated with anti-DIG-HRP for 1 h. Finally, the cells were stained with CY3 and DAPI for 10 min, respectively.

RNA immunoprecipitation (RIP) assays

RIP experiments were performed using the Magna RIP RNA Binding Protein Immunoprecipitation Kit (Millipore) according to the manufacturer's instructions. Briefly, HCC cells were lysed in RIP lysis buffer and then incubated with the RIP immunoprecipitation buffer containing specific antibodies-magnetic beads overnight at 4°C. The beads were collected by magnetic stand and incubated with Proteinase K digestion buffer for 30 min at 37°C with rotation. Finally, the immunoprecipitated RNA was purified and quantified by RT-qPCR.

Dual-luciferase reporter assays

The METTL16 promoter region containing two hypoxia response element (HRE) was constructed into pGL3-based vectors and transfected into HEK-293T cells. All cells were then treated with normoxia or hypoxia for 24 h. After the cells were harvested and lysed, firefly and renilla luciferase activities were measured using the Double-Luciferase Reporter Assay kit (Transgen). The ratio of firefly and renilla luciferase was used to measure promoter activity.

To determine whether Lnc-CSMD1-7 is regulated at the post-transcriptional level by METTL16, pmirGLO-based vectors containing the full length of Lnc-CSMD1-7 (wild type, WT) or two mutated regions (mutant type, MUT) were co-transfected with METTL16 or empty vector into HEK-293T cells for 24 h. Luciferase activity was then measured as previously described.

QUANTIFICATION AND STATISTICAL ANALYSIS

Statistical analysis in this study was performed using SPSS 25.0 (IBM SPSS) and GraphPad Prism 6.0 (GraphPad Software), and all data are presented as mean ± SD. Two groups were compared using unpaired two-tailed Student's *t* test. The expression differences between tumors and paratumors were evaluated using paired two-tailed Student's *t* test. The correlation between Lnc-CSMD1-7 and clinicopathologic characteristics was analyzed by Person chi-squared test. Overall survival (OS) and recurrence free survival (RFS) were display via Kaplan-Meier survival curves and differences were assessed using the log rank test. In addition, univariate and multivariate Cox regression were used to determine the independent risk factors for HCC patients. p values less than 0.05 (*$p < 0.05$, **$p < 0.01$ and ***$p < 0.001$) were considered statistically significant.